JOURNAL OF OPTOELECTRONICS AND ADVANCED MATERILAS, Vol. 10, No. 9, September 2008, p. 2637 - 2643

Growth of nanoislands in thin nickel oxide films

B. SASI, S. SANKAR, K.M. NISSAMUDEEN, GEO RAJAN, A.H. BAHNA, K. G. GOPCHANDRAN*
Department of Optoelectronics, University of Kerala, Thiruvananthapuram-695581, India

Nanostructured, semitransparent and highly conducting nickel oxide thin films were grown on heated substrates kept in vacuum using pulsed laser ablation. Formation of nanoislands, consisting of self-assembly of nanocrystals, following Stranski-Krastanov type growth in thin nickel oxide films is reported. X-ray diffraction studies indicate presence of mixed phases $Ni(OH)_2$, γ-NiOOH, and Ni_2O_3 with grain size 17 nm, in films prepared at 673 K. Films deposited at 773 K showed a resistivity of 3.097×10^{-5} Ω m and transmittance of 46% at 550 nm.

(Received April 4, 2008; accepted August 14, 2008)

Keywords: Oxidation, Nanoisland, Stranski-Krastanov, Microscopy, Transparent conductor, Nickel oxide

1. Introduction

Nanotechnology enables controlled manipulation of matter at or below molecular and supramolecular length scales and aims at commercial utilization. Because of quantum and other size effects, the properties of nano-sized oxide materials differ from those of the bulk [1, 2]. The nonstoichiometry, which varies with the surrounding atmosphere, impurities, and morphologies, is essentially important in transition metal oxides [3]. There has been an increasing interest in developing nanostructured metal oxides with p-type conductivity due to their unique properties and potential applications. Thin films of p-type semiconductors are required in many optoelectronic device applications, which make use of hole injection The properties of p-type oxide thin films are sensitively affected by oxygen pressure [4, 5]. The high metal atom surface-to-volume ratio observed in nanostructured materials not only has importance to the number of active sites in a catalyst, but also can influence oxygen and other anion-defect chemistry and the observation of metastable phases [6].

Nickel oxide is an antiferromagnetic, transition metal oxide, which is considered to be a semiconductor with p-type conductivity and has a wide band gap [7]. It is an attractive material due to its excellent chemical stability, as well as optical, electrical and magnetic properties and is extensively used in electrochromic devices, smart windows, active optical fibers, gas sensors, solar thermal absorbers, electrodes for batteries, p-type transparent conducting electrodes [8-14] etc. A write-once optical recording medium having a recording layer containing mixed oxides of nickel comprising NiO and Ni_2O_3 as a major portion, which is more stable in air compared to other recording layers containing silver oxide or iron oxide has been recently reported [15]. Jean-Michel Caruge et al. explored the possibility of using NiO as hole-transporting layer in the Cd Se quantum dot light emitting devices [16].

The strain driven formation of spatially ordered ensembles of nanoislands recently attracted tremendous attention due to their wide applications in nanotechnology. Fabrication of NiO nanorings [17], hollow spheres and thin films of Ni $(OH)_2$ and NiO with hierarchical structures can also be seen in literature [18]. In this study we report formation of self-assembled islands in nanostructutred nickel oxide thin films. In the present investigation, pulsed laser deposition (PLD) technique is used for the preparation of nanostructured thin nickel oxide films, on heated substrates kept in vacuum. Growth of thin films from atoms deposited from the gas phase is intrinsically a non-equilibrium phenomenon governed by a competition between kinetics and thermodynamics. Precise control of the growth and thus of the properties of deposited films becomes possible only after an understanding of how this competition is achieved [19]. Understanding the exact formation process of an oxide on the nanometer scale will provide fascinating scientific information on the oxidation kinetics of metals. The dependence of size, structure, composition, surface morphology and electrical and optical properties of nanostructured nickel oxide thin films on substrate temperature are also discussed in this paper.

2. Experimental methods

Thin nickel oxide films were prepared on amorphous fused quartz substrates by pulsed laser deposition technique, using a Q-switched Nd: YAG laser (Quanta-ray INDI-Series, Spectra physics) at 532 nm, pulse width 8 ns, and repetition frequency 10 Hz. The target-substrate distance was 7 cm and time of deposition, 30 minutes. The target was rotated with constant speed to avoid pitting of target at any given spot and to obtain uniform ablation.

NiO target was prepared from nickel oxide powder of 99.99% purity (Sigma-Aldrich). The powder target was isostatically pressed and sintered at 1173 K for 5 h, to form pellets of diameter 1.4 cm. The chamber was evacuated to a vacuum of 10^{-6} mbar and then films were deposited on heated substrates kept at different temperatures. The structure and crystallinity of the films was investigated by grazing incidence X-ray diffraction (GIXRD), using Siemens D-5000 diffractometer, operated with monochromatic CuK_{α} radiation source (λ=0.15418 nm, 40 KV, 30 m A), and step scanning mode with steps of 0.05^{o} with a scan speed of 4 sec / step. X-ray reflectivity (XRR) technique was used to determine the thickness of the films. The surface morphology and roughness of the films at nanoscale was investigated using atomic force microscopy (AFM) in contact mode with Digital Instruments Nanoscope III and scanning electron microscopy (SEM), using the system Quanta 200. Optical measurements were performed in the wavelength range from 300 to 900 nm, using a double beam UV-VIS spectrophotometer, Jasco-D 550. The resistivity of the films was measured at room temperature (303 K) by the four-probe method employed with a nanovoltmeter model 2182 A and current source meter model 6430 of Keithley make.

3. Results and discussion

3.1 XRR Studies

X-ray reflectivity represents the interference pattern, called Kiessig fringes, of the reflected X-rays from the surface and interfaces of the film and provides a measurement of the thickness of the film [20]. Thickness of the films was determined by fitting the experimental reflectivity pattern with a simulated one using the reflectivity tool Parratt-32 [21]. Fig. 1 shows typical X-ray reflectivity curve of film prepared at a substrate temperature of 673 K, as a function of X-ray momentum transfer (q_z), along with the simulated one. The rounding of the x-ray reflectivity intensity observed near critical wave vector is due to high X-ray absorption coefficient of Nickel. The fall of reflectivity after the critical wave vector and the damping of oscillation indicate the degree of roughness at the surface and interface of the film [22]. The thickness of the films deposited at substrate temperatures 303, 573, 673 and 773 K as determined by XRR are 32, 13, 10 and 8 nm respectively. The decrease in thickness with increase of substrate temperature may be due to re-evaporation of film material and diffusion of the material resulting from induced softness of the substrate at elevated temperatures. Further the growth of the oxide layer is limited by the rate at which oxygen appears below the nickel oxide layer [23].

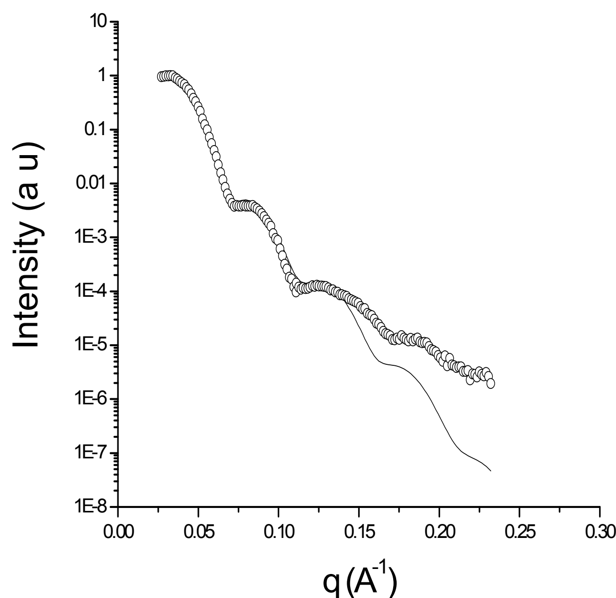

Fig.1 X-ray reflectivity with curve fitting for film deposited at a substrate temperature of 673 K.

3.2 XRD Studies

Fig. 2 shows the GIXRD patterns of thin nickel oxide films deposited at different substrate temperatures. The peaks are indexed according to ASTM data cards of Ni_2O_3 (14- 481), Ni $(OH)_2$ (14-0117) and γ-NiOOH (06-75). No peak corresponding to NiO was found in these patterns. The XRD spectrum of film deposited at 303 and 573 K shows only a weak diffraction peak from (200) plane of Ni_2O_3. The Bragg reflections seen in the diffractograms of films deposited at lower temperatures are broad, indicative of smaller particle sizes and poor crystallinity. When the substrate temperature is increased to 673 K, the intensity of the (200) peak of Ni_2O_3, at 2θ = 44.85 degree is found to increase sharply. This may be due to the enhanced oxidation kinetics and improvement in crystallinity. The films are found to be brown in color and are due to the presence of Ni^{3+} ions in the Ni_2O_3 assignment, acting as color centers [6]. The grain size of the crystallites was calculated for the (200) peak using Scherrer's formula,

$$D = \frac{0.9\lambda}{B Cos\,\theta} \quad (1)$$

where λ, is the wavelength of X-rays, θ the Bragg's angle of the XRD peak and B, the full width at half maximum (FWHM) of the peak. The calculated grain size was 17 nm for the film deposited at 673 K.

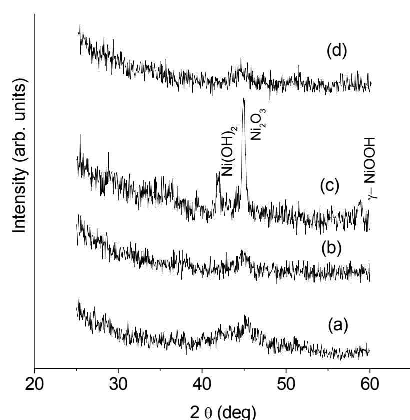

Fig. 2. GIXRD patterns of films deposited at different substrate temperatures: (a) 303, (b) 573, (c) 673 and (d) 773 K.

The peaks appearing at 2θ = 41.86 and 58.75 degree in the film deposited at 673 K can be assigned to nickel hydroxide ($Ni(OH)_2$) and nickel oxide hydroxide (γ-NiOOH) respectively. When the substrate temperature is increased to 773 K, only a broad peak with very small intensity appeared at 2θ ~ 44.7 degree. The driving force for oxidation of a given metal depends on the free-energy change for oxide formation. However, the rate of oxidation and the morphological changes during oxidation depend on complex kinetics, and micro structural considerations, not necessarily solely on thermodynamics. There exists a correlation between the concentration of oxygen deficiency in the nickel oxide lattice and rate of oxide reduction [24]. The presence of large number of vacant lattice sites and local lattice disorders may lead to obvious reduction or even disappearance in intensities of XRD peaks of some lattice planes.

3.3 AFM and SEM Studies

AFM and SEM images of the films prepared at different substrate temperatures are shown in figure 3 and 4 respectively. Formation of nanoislands following Stranski-Krastanov type growth [25] can be seen in the AFM images. The SEM image of the films prepared at 773 K indicates uniform distribution of homogeneous and closely packed crystallites in regions where the islands are absent. Numbers of islands formed in the surface of films deposited at low temperatures (<573 K) were very few. Figure 5 shows the islands in different stages of its growth in two and three dimensions. The number of islands formed is found to be more in films prepared at a substrate temperature of 673 K. Agnoli et al. reported formation of three-dimensional strained islands resulting from a Stranski-Krastanov growth behavior in ultra thin nickel oxide films [26]. Although a grain boundary often is conceived as a two dimensional dividing surface, it is now known that grain boundary cores can spread into complex, three-dimensional configurations of nanometer-scale width. The plastic behavior of crystalline materials is mainly controlled by the nucleation and motion of lattice dislocations. Shan et al reported that in nanocrystalline nickel films with an average grain size of about 10 nm, the grain boundary-mediated processes have become a prominent deformation mode and trapped

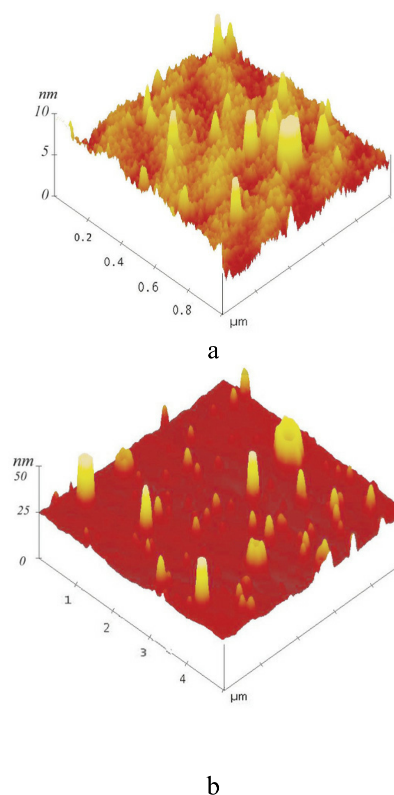

Fig. 3. AFM images of films deposited at substrate temperatures of (a) 673 and (b) 773 K

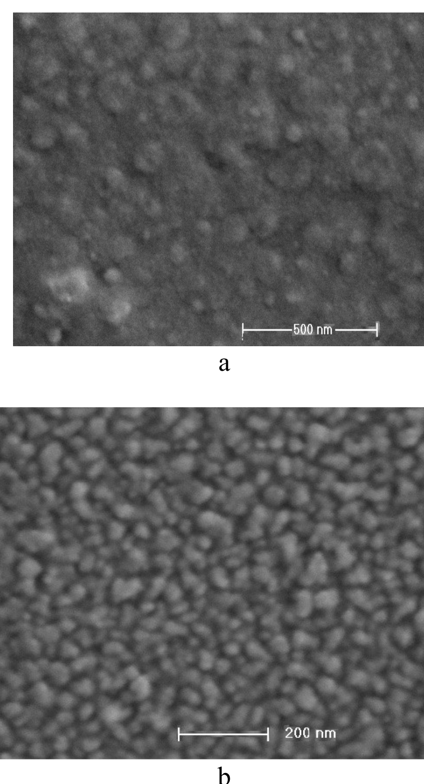

Fig. 4. SEM images of films deposited at (a) 573 and (b) 773 K.

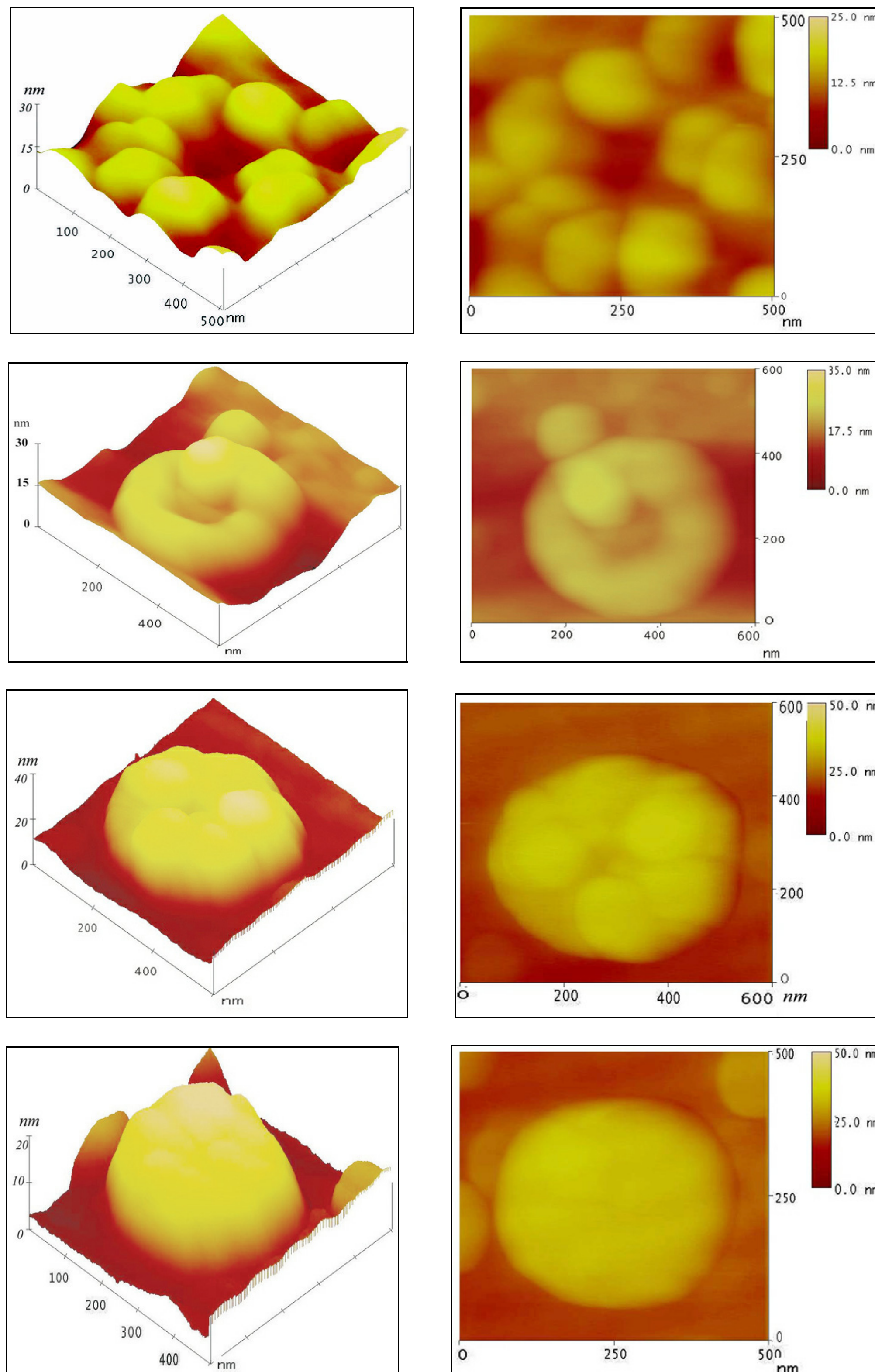

Fig. 5 AFM images (3D and 2D) of the islands in different stages of its growth.

lattice dislocations are observed in individual grains following deformation [27]. They also reported that very high local stress is necessary for the nucleation of partial dislocation in nanocrystalline nickel. The dominance of either a homogeneous or a heterogeneous manner in the nucleation stage of a system is determined by the driving force for nucleation and the interface energy caused by formation of a new phase in a matrix phase [28]. The interface energy is the surface energy of the island, and in the present study it varies little with increase of substrate

temperature above 573 K, since the morphology of islands formed at substrate temperatures 573 and 673 K is almost the same. Therefore, dominance of the nucleation manner should be explained on consideration of the driving force and its kinetic limitation [29]. On the other hand, it has been reported that island formation is greatly suppressed by low-temperature growth [25]. This result strongly suggests that lowering the growth temperature kinetically limits the driving force for island formation. The collapse of islands at its extremity due to release of strain energy [30] can also be seen in the AFM images. Absence of island formation in annealed Ni/NiO films [31, 32] indicates the role of temperature, in island formation, during the growth of film.

3.4 Optical and electrical properties

The spectral transmittance of the nickel oxide films deposited at different substrate temperatures are shown in figure 6. Generally an increase in transmittance can be seen with increase of substrate temperature but reverse is the case for the film deposited at 673 K. This anomalous change may be due to the formation of new phases, Ni $(OH)_2$ and (γ-NiOOH), as seen in XRD spectrum shown in figure 2. The films deposited at 773 K showed an average transmittance of 46% at 550 nm. The optical band gap E_g and absorption coefficient α of the film are connected by the relation [33],

$$\alpha h\nu = A(h\nu - E_g)^m, \quad (2)$$

where A is a constant, hν is the incident photon energy and the exponent m depends on the nature of optical transition. The value of m is ½ for direct allowed, 2 for indirect allowed, 3/2 for direct forbidden and 3 for indirect forbidden transitions [34]. The absorption coefficient has been calculated from the Lamberts formula,

$$\alpha = \frac{1}{t}\ln\left(\frac{1}{T}\right) \quad (3)$$

where T and t are the transmittance and thickness of the films respectively.The band gap of the films was determined using equation (2), assuming a direct transition between bands and is given in table 1. A typical plot of $(\alpha h\nu)^2$ versus photon energy (hν) for the film prepared at a substrate temperature of 673 K is shown in figure 7. It can be seen that both deposition rate and band gap of the films are sensitive to substrate temperature. For very thin films the grain size will be so small that substantial smearing of the band edges is to be expected. Interference effects are also observed.

The electrical conductivity of nickel oxide films depend on their structure and composition and consequently on the deposition environment. The film prepared at 303 K exhibit metallic like conductivity. The resistivities of the films prepared at different substrate temperatures are given in table 1 and the values

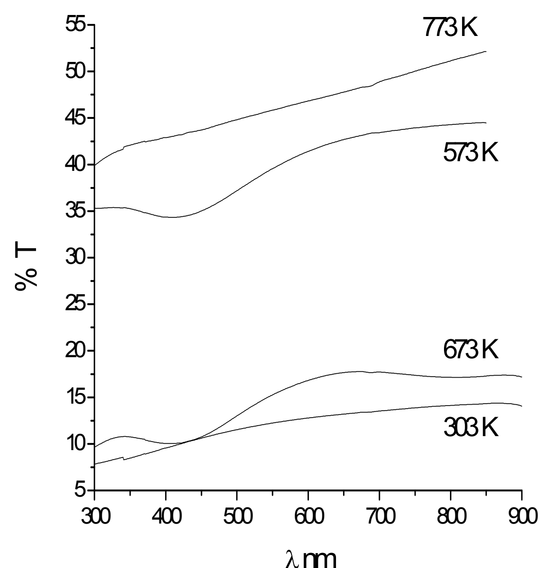

Fig. 6. Transmission spectra of films prepared at different substrate temperatures

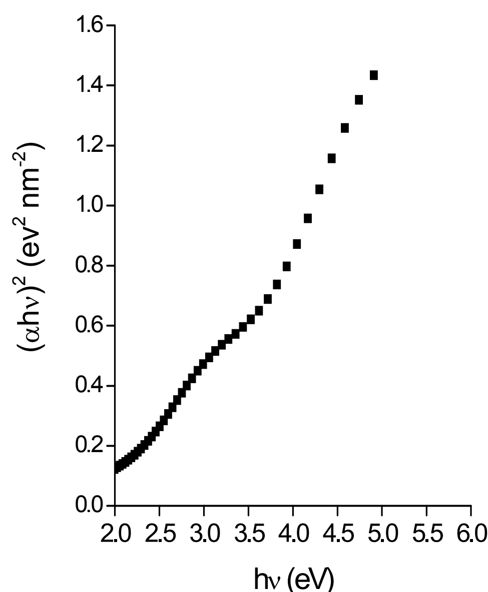

Fig.7. Typical plot of $(\alpha h\nu)^2$ versus photon energy (hν) for the film prepared at a substrate temperature of 673 K.

are found to be lower than the other reported values [35, 36]. Since Ni^{3+} ions of NiOOH and/or Ni_2O_3 are produced as color centers in films of NiO_x with the main frame like NiO structure, it is considered that the colored films behave like a p-type semiconductor and then show lower resistance [37]. Increasing the Ni^{3+} ion concentration as a result of nickel vacancies and/or interstitial oxygen can lower the resistivity of nickel oxide film [38]. The low resistivity obtained for film prepared at 673 K compared

Table1. Optical and electrical properties of nickel oxide films prepared at different substrate temperatures.

Substrate Temp (K)	Thickness nm	Transmittance at 550 nm	Band gap eV	Resistivity Ω m
303	32	9	3.55	-
573	13	40	2.01	4.862×10^{-6}
673	10	16	2.78	7.68×10^{-7}
773	8	46	3.09	3.097×10^{-5}

to other samples may be due to reduction in grain boundary scattering [39] and the defect structure of the films as observed in the XRD studies. The increase in resistivity found for films prepared at high temperatures can be due to reduction in nickel vacancies arising from insufficient oxygen and reduction in film thickness. Since film formation is a non-equilibrium phenomenon governed by a competition between kinetics and thermodynamics, the absence of oxygen during film formation leads to domination of thermodynamic effect at high temperatures.

4. Conclusion

Preparation of semi-transparent and highly conducting ultra thin nickel oxide films on heated substrates kept in vacuum using pulsed laser ablation is reported. Growth of nanoislands in nickel oxide thin films is described with AFM images. The band gap of the films is found to be sensitive to substrate temperature. The film prepared at a substrate temperature of 773 K, in this study show a very low resistivity of 3.097×10^{-5} Ω m and a transmittance of 46% at 550 nm.

Acknowledgement

The work was supported by the Kerala State Council for Science Technology and Environment. We gratefully acknowledge UGC-DAE Consortium, Indore Centre, for the measurements.

References

[1] K.J. Kjabunde, J. Stark, O. Koper, C. Mohs, G.P. Dong, S. Decker, Y. Jiang, I. Lagadic, D. Zhang, J. Phys. Chem. **100**, 12142 (1996).
[2] K. Nomura, H. Ohta, K. Ueda, T. Kamiya, M. Hirano, H. Hosono, Science **300**, 23 (2003).
[3] H.H. Kung, Transition metal oxides, Elsevier, Amsterdam (1989).
[4] B. Sasi, K.G. Gopchandran, Sol. Energy Mater. Sol. Cells **91**,1505 (2007).
[5] N. Uekawa, K. Kancko, J. Phys. Chem. **100**, 4193 (1996).
[6] Jackie Y. Ying. Nanostructured Materials, Academic press, New York, (2001).
[7] H. Kamal, E.K. Elmaghraby, S.A. Ali, K. Abdel-Hady, J. Cryst. Growth. **262**, 424 (2004).
[8] J. He, H. Lindstrom, A. Hagfeldt, S.E Lindquist, J. Phys. Chem. B.**103**. 8940 (1999).
[9] K. Yoshimura, T. Miki, S. Tanemura, Jpn. J. Appl. Phys. **34**, 2440 (1995).
[10] K. Liu, M. Anderson, J. Electrochem. Soc. **143**, 124 (1966).
[11] I. Hotovy, V. Rehacek, P. Siciliano, S. Capone, L. Spiess, Thin solid films **418**, 9 (2002).
[12] J.G. Cook, F.P. Koffyberg, Solar Energy Mater. **10**, 55 (1984).
[13] R.C. Makkus, K. Hemmes, J.H.W.D. Wir, J. Electrochem. Soc. **141**, 3429 (1994).
[14] I.M. Chan, T.Y. Hsu, F.C. Hong, Appl. Phys. Lett. **81**, 1899 (2002).
[15] Hung-Lu Chang, Tzuzn-Ren Jeng, Jung-Po Chen, Wen-Hsin Yen, Pofu Yen, Derray Huang, Jau-Jiu Ju, Jpn. J. Appl. Phys. **44**, 6109 (2005).
[16] Jean-Michel Cruge, Jonathan E. Halpert, Vladimir Bulovic, Moungi G. Bawendi, Nano Lett. **6**, 2991(2006).
[17] Dingsheng Wang, Run Xu, Xun Wang, Yadong Li, Nanotechnology **17**, 979 (2006).
[18] Debao Wang, Caixia Song, Zhengshui Hu, Xun Fu, J. Phys. Chem. B **109**, 1125 (2005).
[19] Zhenyu Zhang, Max G. Lagally, Science **276**, 377 (1997).
[20] L.G. Parratt, Phys. Rev. **95**, 359 (1954).
[21] Christian Braun, Hahn Meitner Institut, Berlin, Parratt-32.
[22] S. Banerjee, M.K. Sanyal, A. Datta, A. Kanakraju, S. Mohan, Phys. Rev. B. **54**, 16377 (1996).
[23] M.R. Fitzsimmons, T.J. Silva, T.M. Crawford, Phys. Rev. B. **73**, 14420 (2006).
[24] Jose A Rodriguez, Jonathan C. Hanson, Anatoly I. Frenkel, Jae Y. Kim, Manuel Perez, J. Am. Chem. Soc. **124**, 346 (2002).
[25] O.G. Schmidt, O. Kienzle, Y. Hao, K. Eberl, F. Ernst, Appl. Phys. Lett. **74**, 1272 (1999).
[26] S. Agnoli, A. Barolo, P. Finetti, F. Sedona, M. Sambi, G. Granozzi, J. Phys. Chem. C **111- 9**, 3736 (2007).
[27] Z. Shan, E.A. Stach, J.M.K. Wiezorek, J.A. Knapp, D.M. Follstaedt, S.X. Mao, Science **305**, 654 (2004).
[28] R.D. Doherty, Physical Metallurgy, edited by R.W. Cahn, P. Haasen, North- Holland, Amsterdam (1983).
[29] A. Sakai, T. Tatsumi, Phys. Rev. Lett. **71**, 4007 (1993).

[30] F. Carlier, S. Benrezzak, Ph. Cahuzac, N. Kebaili, A. Masson, A.K. Srivastava, C. Colliex, C. Brechignac, Nano Lett. **6**, 1875 (2006).
[31] B. Sasi, K.G. Gopchandran, Nanotechnology **18**, 115613 (2007).
[32] B. Sasi, K.G. Gopchandran, P.K. Manoj, P. Koshy, P. Prabhakara Rao, V.K. Vaidyan, Vacuum. **68**, 149 (2002).
[33] J. Tauc, Amorphous and Liquid Semiconductors, Plenum, London (1974).
[34] J.I. Pankove, Optical Processes in Semiconductors, Prentice-Hall, Englewood Cliffs, N J (1971).
[35] P.S. Patil, L.D. Kadam, Appl. Surf. Sci. **199**, 211 (2002).
[36] H. Sato, T. Minami, S. Takata, T. Yamada, Thin solid films **236**, 27 (1993).
[37] M. Kitao, K. Izawa, K.Urabe, T. Komatsu, S. Kuwano, S. Yamada, Jpn. J. Appl. Phys. **33**, 6656 (1994).
[38] Y.M. Lu, W.S. Hwang, J.S. Yang, H.C. Chuang, Thin solid films **420**, 54 (2002).
[39] K.G. Gopchandran, B. Joseph, J.T. Abraham, P. Koshy, V.K. Vaidyan, Vacuum **48**, 547 (1997).

*Corresponding author: gopchandran@yahoo.com